Surface crack growth prediction under fatigue load using the S-version Finite Element Model (S-FEM)

Surface crack growth prediction under fatigue load using the S-version Finite Element Model (S-FEM)

M N M Husnain[1], M R M Akramin[1] and Z L Chuan[2]

[1]Faculty of Mechanical Engineering, Universiti Malaysia Pahang, 26600 Pekan, Pahang Darul Makmur
[2]Faculty of Industrial Sciences & Technology, Universiti Malaysia Pahang, Lebuhraya Tun Razak, 26300 Gambang, Pahang Darul Makmur

*Corresponding author: husnainoh94@gmail.com

Abstract. Prediction of fatigue crack growth is one of the vital issues to prevent catastrophic failure from damage tolerance perspective. The surface of crack shape usually in semi-elliptical that maintained during the whole propagation. The investigation of this paper is to illustrate the surface crack growth that subjected to fatigue loading. The four-point bending and three-point bending have been simulated by using the S-version Finite Element Model (S-FEM). The simulation is conducted for aluminium alloys A7075-T6 and A2017-T3 with all of the parameters based on the previous experiment. The semi-elliptical crack shape is applied during the simulation process to represent with the reality of crack growth phenomena. Paris' Law model approach is presented in fatigue crack growth simulation. The S-FEM produced the surface crack growth and fatigue life prediction. The results of the S-FEM prediction then compared with the previous experiments. The results presented in a graph for comparison between S-FEM prediction with the experimental results. The S-FEM results obtained is good agreement with the experiment results.

1. Introduction

The defects play an important role in imparting properties to materials. Defects on the materials for instances initial cracks or imperfections that could happen to the materials is important to be studied. The crack normally affected mechanical behaviors and structures of materials as defect. Then, the performances and components of the materials are changed naturally. The best word that can describe the crack also known flaw. Crack is formed from the initial flaw in materials structure when load is applied. When the flaw reaches a critical size, the crack may propagate in this condition. The catastrophic failure is presented in the materials component [1]. Nowadays, an indication of initial flaws is the main source that affecting the structural materials. It is produced by impact for the critical failure in the engineering industries for instance automotive, aerospace and others. Initial flaw size of the crack growth is one of the factor for the failure occurred. The initial flaws size can be modeled to investigate the fatigue life of the materials [2], [3]. The fatigue crack growth model is simulated with the numerical method using the powerful computational tools.

Fatigue crack growth an embedded crack is studied with some parameters likes crack shapes, sizes and stress ratio. It is to investigate the fatigue crack growth behavior of interacting cracks. The crack growth is simulated by using the finite element method (FEM). It is able to characterize an arbitrary crack in FEM with meshing. The initial crack is beginning of degradation at crack initiation. The

simulation can meet the criterion of crack initiation when it started [4]. The computational effort becomes very large when the iterations of crack propagation increase. Extended FEM is used to avoid mesh dependent difficulties in the modeling of crack growth problems. It is used as the partition of unity enrichment [5]. The function of the shape in FEM is the most vital enrichment function. FEM application in LEFM has formed the enrichment function as well as singular crack tip expansion functions. It is used to define the displacement or stress contours with a 3D crack in an elastic medium accurately. The global error is controlled by the quality of local error. If the local error is presented in high enrichment function, it is expected good global accuracy as well [6]. The meshing problems and difficulties of embedded crack shape is resolved with some improvements in FEM.

The extended version can be applied to improve the quality of FEM calculations by using the existing adaptive techniques such as h-version and p-version. The h-version is used for mesh refining and the p-version is used for increased the polynomial order. The finite element mesh based on the h-version has subdivided the elements in the same order into the small elements. It is purposed to get fine the in the meshing of the elements. The p-version is used to increase the polynomial order approximation in the same mesh [7]. The p-version lefts the mesh unchanged and increases the polynomial degree of the shape functions locally or globally [8]. Lastly, the combination for both of them can increase the polynomial degree and mesh refinement. It is called as S-version that has a great advantage to utilize [9], [7], [10]. The S-version has increased the resolution the higher order hierarchical elements by superimposing additional meshes. The s-version is implemented in FEM as S-FEM to solve the various problems. The S-FEM is applied on surface crack growth to know its lifetime and crack propagation based on it parameters [11].

In numerical method, the problem is about meshing process between the model with the initial crack shape. The prediction of fatigue life is difficult to compute when the fracture start propagates and failure. This paper presents the analysis of S-FEM for fatigue surface crack. The objective of this paper is to illustrate the surface crack growth under bending fatigue loads. The fatigue life is computed and presented in this paper simultaneously. The S-FEM is used as a method to solve the fatigue crack growth for the fatigue crack growth model. In this study, the results from the S-FEM simulation for four-point bending and three-point bending is compared with previous researcher's experimental results.

2. Materials

The Aluminium alloy A7075-T6 is used for aircraft parts in the aircraft industry. The aluminum alloy was a ductile metal which can be easily formed while being resistant to loads and stress. The aluminium alloy with zinc as the primary alloying element. It was strong with strength comparable to many sheets of steel, and had good fatigue strength and average machinability. The 7075 aluminum alloy's composition roughly includes 5.6 - 6.1 % zinc, 2.1 - 2.5 % magnesium, 1.2 - 1.6 % copper, and less than a half percent of silicon, iron, manganese, titanium, chromium, and other metals. Table 1 shows the parameter detail for four-point bending of Aluminium alloy A7075-T6.

Table 1. Input for Aluminium alloy A7075-T6 from Ohdama et al. [12].

Variable	Value
Critical stress intensity factor, K_{IC}	29 MPa·√m
Fatigue power parameter, n	2.88
Tensile Strength, Yield	691 MPa
Young's modulus, E	71.7 GPa
Paris coefficient, C	6.54×10^{-13}
Threshold value, ΔK_{th}	5.66 MPa·√m
Maximum crack growth increment, da_{max}	1.3 mm
Initial crack length, c	4.5 mm
Initial crack depth, a	3.5 mm

Aluminium alloy A2017-T3 is widely used commonly in the manufacture of aircraft components, screw machine products and fittings, pulleys, gauges, coat hangers, and in crochet and knitting needles. The chemical composition of Aluminium alloy A2017-T3 was included 91.5 - 95.5 % aluminium, 3.5 - 4.5 % copper, 0.7 % iron, 0.4 - 1 % manganese, 0.4 - 0.8 % magnesium, 0.2 - 0.8 silicon, 0.25 % zinc, 0.15 % titanium and 0.1 % of chromium. The input details for Aluminium 2017-T3 three-point bending is shown in the Table 2.

Table 2. Input for the Aluminium alloy A2017-T3 from Kikuchi et al. [13].

Variable	Value
Critical stress intensity factor, K_{IC}	26 MPa·√m
Fatigue power parameter, n	2.93
Tensile Strength, Yield	333 Mpa
Young's modulus, E	70.2 Gpa
Paris coefficient, C	2.66×10^{-10}
Threshold value, ΔK_{th}	6.7 MPa·√m
Initial crack length, c	2.85 mm
Initial crack depth, a	5.00 mm

3. Methodology

3.1 Four-point bending and three-point bending

Generally, the S-FEM concepts applied in this simulation to analyze the surface crack growth. The semi-elliptical crack shape introduced at the center of the models [14], [15]. The four-point bending model with $2b$ = 65 mm, $2h$ = 160 mm and t = 25 mm developed in the S-FEM as shown in the Figure 1 (a). The crack propagated based on the simulation until the fracture propagated completely. The semi-elliptical crack shape is located at the center for this specimen model. An initial crack shape aspect is with a = 3.5 mm and $2c$ = 4.5 mm.

By referring to the Figure 1 (b) that shows the details of the dimension for the geometry of three-point bending of Aluminium alloy A2017-T3 with $2h$ = 150 mm, $2b$ = 50 mm and t = 15 mm. The model was simulated in S-FEM by the followed the input parameters. There are three stages of fatigue crack growth. The first one is crack initiation, the second one is fatigue crack propagation and lastly is fatigue failure propagation. The semi-elliptical crack shape as an initial crack was designed with a = 5 mm and $2c$ = 2.85 mm.

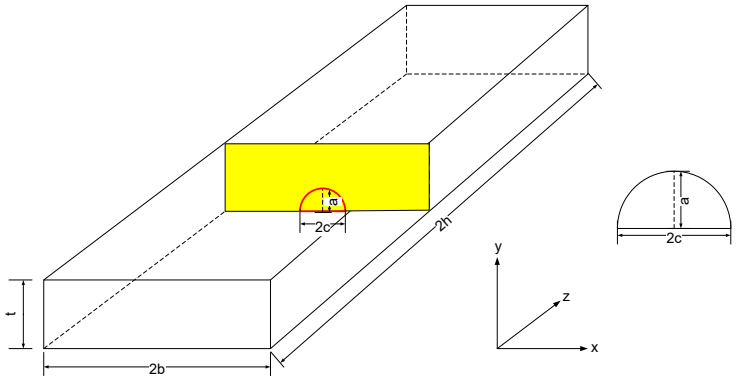

(a) Details dimensions of four-point bending model with a semi-elliptical crack shape for Aluminium alloy A7075-T6.

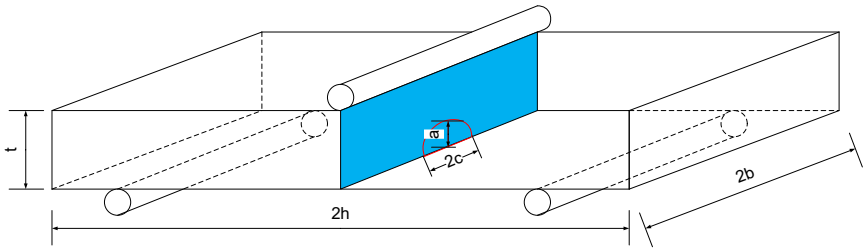

(b) Details dimensions of three-point bending model with a semi-elliptical crack shape for Aluminium alloy A2017-T3.

Figure 1. The geometry of four-point bending of (a) and three-point bending of (b).

Based on the Figure 2 (a) the model for four-point bending is shown in a completely meshing process with a boundary condition such as loads and constraint. The model used 0.1 as stress ratio to produce beach marks at the surface fatigue crack. The model (a) is conducted with 45 kN as a loading in cyclic load. The use of 45kN is to ensure it discovered in fatigue region, which affirmed that the fatigue would occur for the dimensions of this material. The crack shape aspect ratio, *a/c* was 0.8. The three-point bending was shown in Figure 2 (b). The 9 kN as a load is applied repeatedly on the surface model (b) with a stress ratio also 0.1. The crack aspect ratio, *a/c* for the model (b) was 1.7. According to the input parameters to the previous experimental specimens on Table 1 and Table 2. The models simulated in S-FEM for prediction the surface crack and fatigue life.

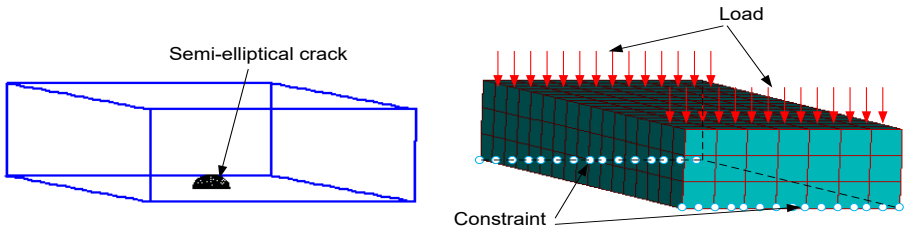

(a) Model four-point bending in S-FEM

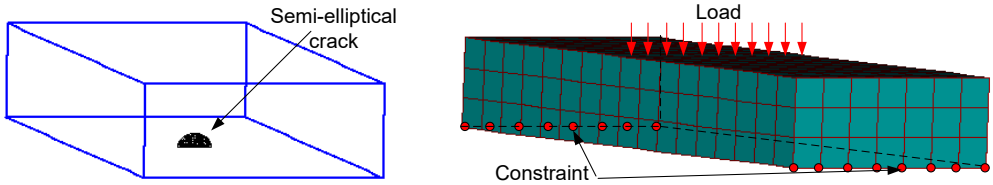

(b) Model three-point bending in S-FEM

Figure 2. Overlaid local mesh in wireframe view and global mesh with boundary condition.

3.2 S-version Finite Element Model (S-FEM)

The concept of S-FEM was exhibited in Figure 3 that implemented on this surface cracks growth analysis. The concept consists of two parts area such as local and global area. These two parts of the area are important to generate the meshing process of the model analysis. The local area was discovered the crack tip meshing and the global area discovered for the whole model.

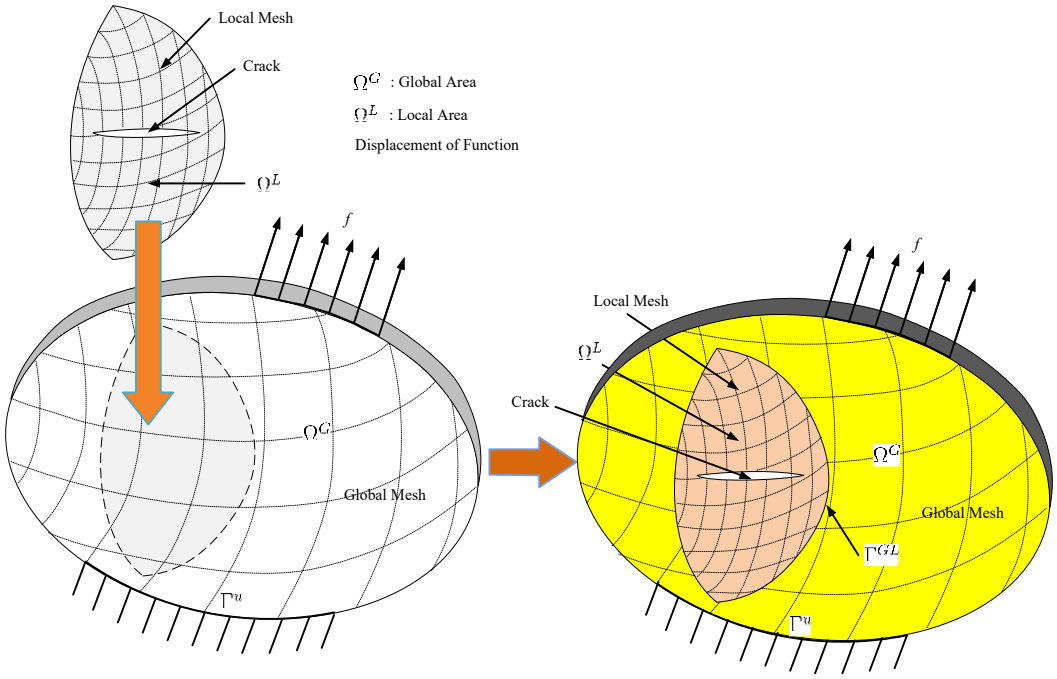

Figure 3. The concept of S-FEM.

The two of parts meshing combined as followed as S-FEM concept. The different orientation of mesh produced such as coarser mesh and finer mesh. The global area generated by coarser mesh and the finer mesh was generated for the local area. The crack tip discovered by the local area during the creation of the local mesh, Ω^L. The global mesh, Ω^G is produced for the whole global area. The local mesh subsequently enveloped onto the global mesh. The boundary of each area represented as Γ. The global area applied by the boundary of constraint displacement, Γ^u, and the boundary of force, Γ^t. The local area embedded in the global area is represented as overlay boundary, Γ^{GL}. The overlay boundary examined to compute the displacement of each node. The displacement in the overlaid area is computed from the local and global meshes as follows:

$$u(x)=\begin{cases}u^G(x) & x\in\Omega^G-\Omega^L\\ u^G(x)+u^L(x) & x\in\Omega^L\end{cases} \tag{1}$$

The strain at the overlaid area is computed by the calculation of the summation from the strain at the local and global area as follows:

$$\varepsilon(x)=\varepsilon^G(x)+\varepsilon^L(x) \tag{2}$$

The equation of principal of virtual work is related to the stress and strain relationship as follows:

$$\begin{aligned}&\int_\Omega\left\{\delta\varepsilon^G\right\}^T[D]\left\{\varepsilon^G\right\}d\Omega^{G-L}-\int_\Gamma\left\{\delta u^G\right\}^T\{f\}d\Gamma^{GL}\\&+\int_\Omega\left(\left\{\delta\varepsilon^G\right\}^T+\left\{\delta\varepsilon^L\right\}^T\right)[D]\left(\left\{\varepsilon^G\right\}+\left\{\varepsilon^L\right\}\right)d\Omega^L\\&-\int_\Gamma\left(\left\{\delta u^G\right\}^T+\left\{\delta u^L\right\}^T\right)\{f\}d\Gamma^L=0\end{aligned} \tag{3}$$

Where Ω^{G-L} represents the non-overlay area. In matrix form, the equation for S-FEM is:

$$\begin{bmatrix} K_{GG} & K_{GL} \\ K_{LG} & K_{LL} \end{bmatrix} \begin{Bmatrix} u^G \\ u^L \end{Bmatrix} = \begin{Bmatrix} F_G \\ F_L \end{Bmatrix} \tag{4}$$

where

$$[K_{GG}] = \int_{\Omega^G} [B^G]^T [D][B^G] d\Omega^G$$

$$[K_{GL}] = \int_{\Omega^L} [B^G]^T [D][B^L] d\Omega^L$$

$$[K_{LG}] = \int_{\Omega^L} [B^L]^T [D][B^G] d\Omega^L$$

$$[K_{LL}] = \int_{\Omega^L} [B^L]^T [D][B^L] d\Omega^L$$

The $[B]$ is the displacement-strain matrix and $[K]$ matrix is the stiffness matrix for local and global in the overlaid area. The nodal force, $\{F_L\}$ at the local area and the nodal force, $\{F_G\}$ at global area respectively. The displacement of each node is calculated by computing the Eq. (4) for both global and local meshes. The local mesh is changed the size and global mesh is not affected for it. The re-meshing process can be generated for a local area alone. The re-meshing process is needed for the fatigue crack growth model. Based on the Figure 2, it shown the combination of local mesh with the global mesh. The combination is applied based on the boundary condition such as loading and constraint. In every iteration, the local mesh crack growth is expanded time by time until the fracture completed. The value of energy release rate is calculated for every new size of local mesh. The stress intensity factor (SIF) obtained based from the calculation of energy release rate.

$$K_I = \sqrt{EG_I}, \quad K_{II} = \sqrt{EG_{II}}, \quad K_{III} = \sqrt{2\mu G_{III}} \tag{5}$$

E is Young's modulus of elasticity under the plane stress condition. For the plain strain condition the equation as follows $E/1\text{-}v^2$.The v is a Poisson's ratio. Fracture is analyzed by using the of linear fracture mechanics concepts; the crack propagation condition is assumed to be based upon the critical energy release rate. The energy release rate utilized in the crack growth analysis.

The Virtual Crack Closure Method (VCCM) is applied in this analysis to determine the energy release rate [16]. The VCCM is examined the crack tip opening displacement that located near to the crack front. The VCCM then been calculated by using the according to the equation:

$$G_{Total} = \frac{1}{2\Delta w^J} \sum_{I=1}^{5} C^I v_i^I P_i^I \tag{6}$$

where I is a nodes number that be located around the crack tip. The nodal force, P_i^I and the opening displacement, v_i^I at the five nodes at the front edge of the crack front. The triangle shape, Δ is the width of the element in the radial direction. The width of the element parallel is w^J to the crack front. The constant C^I is expressed as:

$$\mathrm{C}^1 = \mathrm{C}^2 = \frac{w^J}{w^{J+1} + w^J}, \quad \mathrm{C}^3 = 1, \quad \mathrm{C}^4 = \mathrm{C}^5 = \frac{w^J}{w^{J-1} + w^J}, \tag{7}$$

The crack plane with a certain condition with VCCM implementation. The segments are used to define the displacement and stresses. The areas of the element before, S_2^J and after, S_1^J crack front are expressed as:

$$\begin{aligned} S_1^J &= \int_{\theta_1}^{\theta_2}\int_0^{\Delta}(R+r)drd\theta = \int_{\theta_1}^{\theta_2}\left(\Delta R+\frac{\Delta^2}{2}\right)d\theta \\ S_2^J &= \int_{\theta_1}^{\theta_2}\int_0^{\Delta}(R-\Delta+r)drd\theta = \int_{\theta_1}^{\theta_2}\left(\Delta R-\frac{\Delta^2}{2}\right)d\theta \end{aligned} \tag{8}$$

The energy release rate, implemented by [16]. The equations are shown below:

$$G_I = \frac{K_I^2}{E} = \frac{1}{2\left[S_1^J-\frac{1}{4}\left(S_1^J-S_2^J\right)\right]}\int_{S_1^J}\sigma_{33}(r)v_3(\Delta-r)\,dS_1^J \tag{9}$$

$$G_{II} = \frac{1}{2\left[S_1^J-\frac{1}{4}\left(S_1^J-S_2^J\right)\right]}\int_{S_1^J}\sigma_{31}(r)v_1(\Delta-r)\,dS_1^J \tag{10}$$

$$G_{III} = \frac{1}{2\left[S_1^J-\frac{1}{4}\left(S_1^J-S_2^J\right)\right]}\int_{S_1^J}\sigma_{32}(r)v_2(\Delta-r)\,dS_1^J \tag{11}$$

$$G_{Total} = \frac{1}{2\left[S_1^J-\frac{1}{4}\left(S_1^J-S_2^J\right)\right]}\int_{S_1^J}\sigma_{3i}(r)v_i(\Delta-r)\,dS_1^J \tag{12}$$

where v_i is the crack opening displacement at the crack face and σ_{3i} is the cohesive stress at the local axis, x_3. Then, the energy release rate can be converted to the ΔK_{eq} via Eq.(5). The crack growth rate is expressed by Paris's law equation as follows:

$$\frac{dn}{dN} = C\left(\Delta K_{eq}\right)^n \tag{13}$$

Where N and da are the number of cycles and crack growth increment, respectively. C and n coefficients are material constants. The crack length is presented as:

$$da = C\left(\Delta K_{eq}\right)^n \times dN \tag{14}$$

The ΔK_{eq} is the equivalent SIF. It is a parameter that associated with the fatigue crack growth rate under mixed-mode conditions. The equivalent SIF ΔK_{eq} is presented by:

$$\Delta K_{eq} = \frac{\Delta K_I}{2}+\frac{1}{2}\sqrt{\Delta K_I^2+4\left(1.155\Delta K_{II}\right)^2+4\left(\Delta K_{III}\right)^2} \tag{15}$$

The crack growth angle, φ_o is influenced by the value of K_I, K_{II}, and K_{III}. Based on Richard et al. [17], the crack growth angle can be calculated as follows:

$$\varphi_o = \mp\left[\frac{|K_{II}|}{K_I + |K_{II}| + |K_{III}|} - 70^\circ \left(\frac{|K_{II}|}{K_I + |K_{II}| + |K_{III}|} \right)^2 \right] \tag{16}$$

where $\varphi_o < 0^\circ$ for $K_{II} > 0$ and $\varphi_o > 0^\circ$ for $K_{II} < 0$ and $K_I \geq 0$.

4. Results and discussion

Figure 4 illustrated the beach marks for the surface crack growth of four-point bending and three-point bending model. Fracture surface is propagated when it reached a critical size. The models produce six beach marks based on their cycles of fatigue loading.

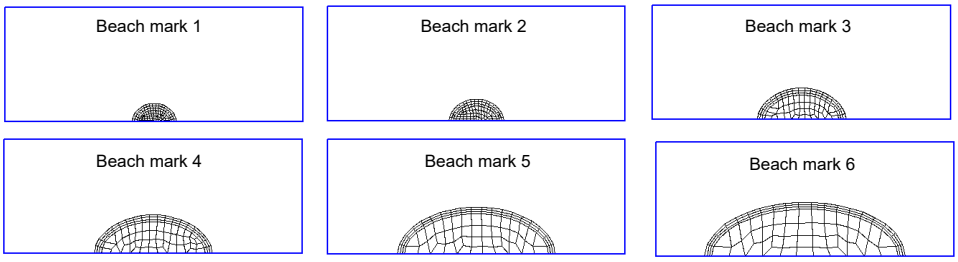

(a) Surface crack for four-point bending.

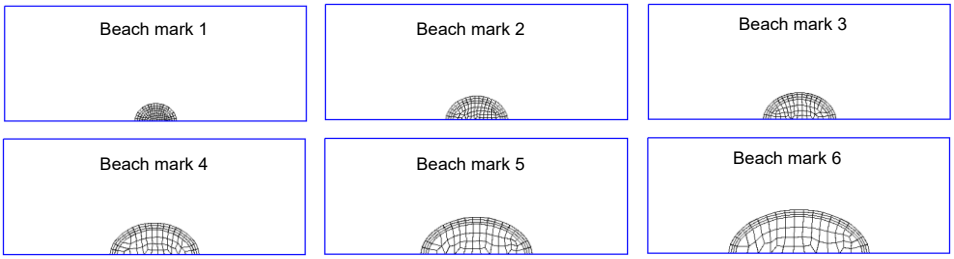

(b) Surface crack for three-point bending.

Figure 4. The beach marks for surface fatigue crack.

Figure 5 shows the crack depth, *a* versus crack length, *c* in the fatigue crack propagation. The surface crack from the four-point bending experiment produces five beach marks. The line of beach marks is presented in the graph by its coordinate for a comparison. The crack is propagated from the initial flaws until completely fracturing. The S-FEM are produces another beach marks to compare with experiment. Based on the results obtained, it has been observed that the beach marks for experiment between S-FEM slightly different. The initial beach marks for S-FEM was marginally similar as the experiment and changed slightly until it fractures. The point of crack length for S-FEM was slightly differences between surface crack from the experiment. While the point of crack depth for S-FEM is moderately far apart from the experiment. In the overall graph, the S-FEM result is valid with experiment results. The surface fatigue crack is computed by following Paris's law theory which stated in Eq. (15) and (16).

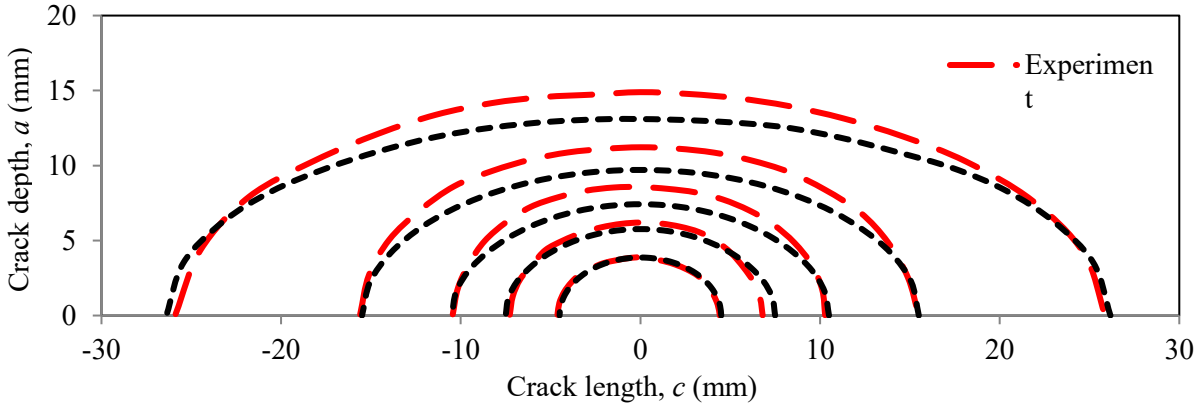

Figure 5. The comparison surface cracks for four-point bending between Ohdama et al. [12] experiment.

The crack length, c versus the cycles, N where a time period to crack propagate until it failure is shows in Figure 6. The fatigue life comparison from experiment between S-FEM is illustrated in Figure 6. The S-FEM is reached a maximum point at 20 mm crack length with 136382 cycles. While the experiment is reached a maximum point at 20 mm for crack length with 473367 cycles. There are significant differences of a maximum point between S-FEM and experiment. The S-FEM fatigue life is quickly reached a failure compare with the experiment. So the numerical method is investigated in code S-FEM at part of Paris' Law equation. The S-FEM calculated the higher value of stress intensity factor (SIF) for mode I, so due to that fact the prediction fatigue life becomes shorter. The value of SIF in S-FEM is difficult computation at the nodes of three dimensional crack front.

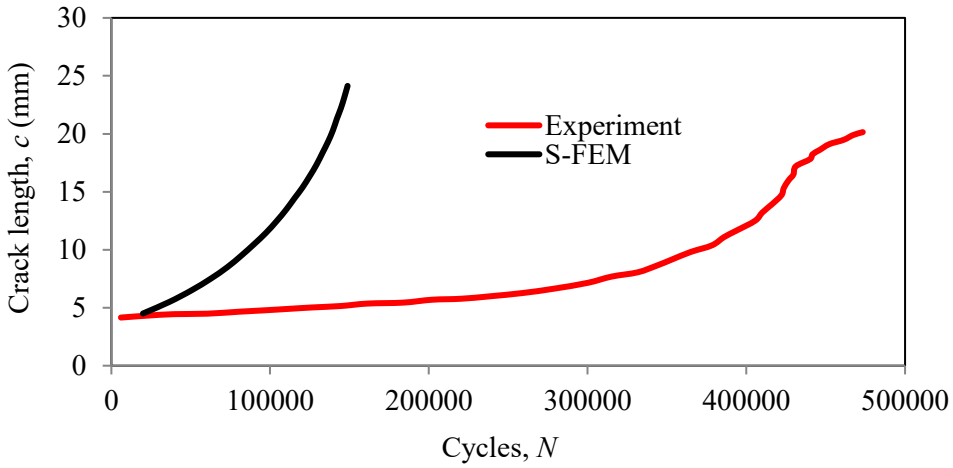

Figure 6. The fatigue life of four-point bending.

The experiment result from Kikuchi et al. [13] is presented to compare with S-FEM result for fatigue life of Aluminium 2017-T3 in three-point bending. The Figure 7 illustrated the fatigue life with the crack length, c versus cycles, N until it failure crack propagation. The S-FEM result is achieved maximum point at 14 mm of crack length and 44463 N of cycles. Then, the experiment is reached a maximum point at 14 mm of crack length with 43856 N of cycles. The comparison of S-FEM and experiment are slightly accurate as a prediction. So, the meshing process for global and local are seemly corrected when simulated in S-FEM.

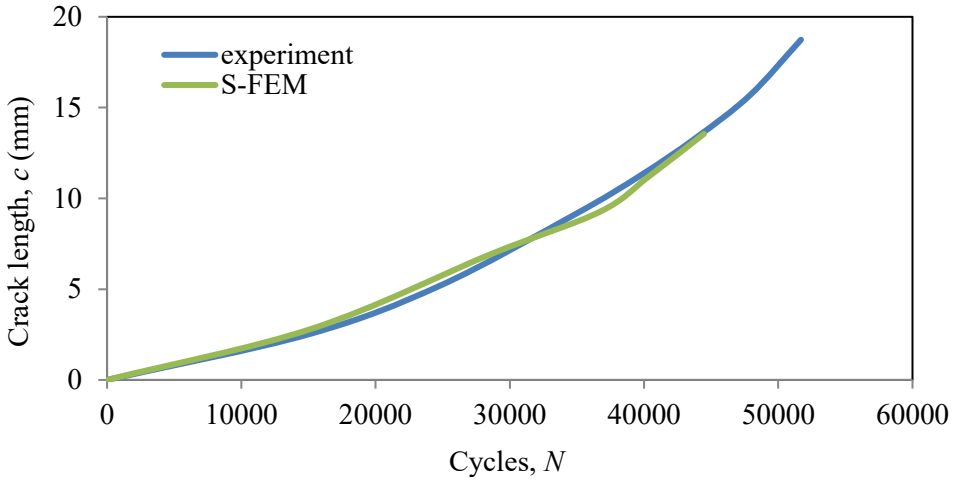

Figure 7. The fatigue life of Aluminium 2017-T3.

5. Conclusions

The crack growth surface is simulated by S-FEM and it is useful for prediction of a surface fatigue crack. The beach marks are produced from the S-FEM agreed with the experiment beach mark. Besides that, the fatigue life of four-point bending is significant differences among experimental result. The numerical method or meshing process is closely related despite due to the fact. The code in S-FEM must be re-checked if there have an incorrect parameters and values. Then, the three-point bending is produced a slightly differences result compared with the experimental result. The fatigue life result from S-FEM for three-point bending is agreed with the experiment fatigue life result. It is concluded the model of S-FEM for four-point bending has distorted in meshing or error in S-FEM coding. Further investigations of the numerical method in S-FEM are required to extend the present work.

Acknowledgments

This study was funded by RDU170383 from Universiti Malaysia Pahang (UMP) and Fundamental Research Grant Scheme (FRGS/1/2017/TK03/UMP/02/24) from Kementerian Pendidikan Malaysia (KPM) with number RDU170124.

References

[1] Kamaludin, M.A., et al.,2017 A fracture mechanics approach to characterising the environmental stress cracking behaviour of thermoplastics. *Theoretical and Applied Fracture Mechanics*. **92**: p. 373-380.

[2] Ma, C., et al.,2017 An effective computational approach based on XFEM and a novel three-step detection algorithm for multiple complex flaw clusters. *Computers & Structures*. **193**: p. 207-225.

[3] Nilsson, K.F., N. Taylor, and P. Minnebo,2006 Analysis of fracture tests on large bend beams containing an embedded flaw. *International Journal of Pressure Vessels and Piping*. **83**: p. 72-83.

[4] Zhang, Y., Z. Xiao, and J. Luo,2017 Fatigue crack growth investigation on offshore pipelines with three-dimensional interacting cracks. *Geoscience Frontiers*.

[5] Feng, S.Z. and W. Li,2018 An accurate and efficient algorithm for the simulation of fatigue crack growth based on XFEM and combined approximations. *Applied Mathematical Modelling*. **55**: p. 600-615.

[6] O'Hara, P., C.A. Duarte, and T. Eason,2016 A two-scale generalized finite element method for interaction and coalescence of multiple crack surfaces. *Engineering Fracture Mechanics*. **163**: p. 274-302.

[7] Fish, J.,1992 The s-version of the finite element method. *Computers & Structures*. **43**: p. 539-547.

[8] Düster, A. and E. Rank,2001 The p-version of the finite element method compared to an adaptive h-version for the deformation theory of plasticity. *Computer Methods in Applied Mechanics and Engineering*. **190**: p. 1925-1935.
[9] Babuška, I. and M. Suri,1990 The p- and h-p versions of the finite element method, an overview. *Computer Methods in Applied Mechanics and Engineering*. **80**: p. 5-26.
[10] Schmidt, A. and K.G. Siebert,2000 A posteriori estimators for the h – p version of the finite element method in 1D. *Applied Numerical Mathematics*. **35**: p. 43-66.
[11] Kikuchi, M., Y. Wada, and K. Suga,2011 Surface crack growth simulation under mixed mode cyclic loading condition. *Procedia Engineering*. **10**: p. 427-432.
[12] Ohdama, C., *Effect Of KIII On Fatigue Crack Growth Behavior*, in *Department of Mechanical Engineering*. 2012, Tokyo University of Science, Japan [in Japanese]: Yamazaki, Chiba.
[13] Masanori Kikuchi, Y.W., Maigefeireti Maitireyimu and Hirotaka Sano 2010 Closure Effect on Interaction of Two Surface Cracks Under Cyclic Bending. *ASME 2010 Pressure Vessels and Piping Conference*. **Volume 1**.
[14] McFadyen, N.B., R. Bell, and O. Vosikovsky,1990 Fatigue crack growth of semi-elliptical surface cracks. *International Journal of Fatigue*. **12**: p. 43-50.
[15] Shi, K., et al.,2014 A theoretical model of semi-elliptic surface crack growth. *Chinese Journal of Aeronautics*. **27**: p. 730-734.
[16] Okada, H., et al.,2005 Three dimensional virtual crack closure-integral method (VCCM) with skewed and non-symmetric mesh arrangement at the crack front. *Engineering Fracture Mechanics*. **72**: p. 1717-1737.
[17] Richard, H.A., M. Fulland, and M. Sander,2005 Theoretical crack path prediction. *Fatigue & Fracture of Engineering Materials & Structures*. **28**: p. 3-12.